Photoluminescence excitation study of split-vacancy centers in diamond

E. A. Ekimov,[1] P. S. Sherin,[2,3] V. S. Krivobok,[4] S. G. Lyapin,[1] V. A. Gavva,[5] and M. V. Kondrin[1,*]

[1]*Institute for High Pressure Physics RAS, 108840 Troitsk, Moscow, Russia*

[2]*International Tomography Center SB RAS, 630090, Institutskaya street 3A, Novosibirsk, Russia*

[3]*Novosibirsk State University, 630090, Pirogova street 2a, Novosibirsk, Russia*

[4]*Lebedev Physical Institute RAS, 117942, Leninsky Prospect 54, Moscow, Russia*

[5]*Institute of Chemistry of High-Purity Substances RAS, 603950, Tropinina Street 49, Nizhny Novgorod, Russia*

(Received 22 September 2017; revised manuscript received 8 December 2017; published 17 January 2018)

Two known representatives of the split-vacancy complexes in diamond, the negatively charged silicon-vacancy SiV^- and recently discovered germanium-vacancy GeV^- defects, were comparatively studied for their photoluminescence (PL) and complementary optical absorption spectra. The observed strong difference between luminescence and absorption spectra indicates a strong frequency defect, that is the difference of binding energies of impurity atom in the ground and excited electronic states, in these color centers. The presence of frequency defect is well supported by first-principle calculations. The obtained results accompanied with isotopic effects shed light on the structure of these centers in the ground and excited electronic states that would open the doorway to their theoretical description.

DOI: 10.1103/PhysRevB.97.045206

I. INTRODUCTION

In recent years the split-vacancy complexes in diamond have attracted the attention of researchers as possible candidates for quantum communication networks [1–4]. Here, we will mainly focus on the well-studied negatively charged SiV^- center [5–13] and compare it with the recently discovered GeV^- center [14–17]. Both centers can be produced in nano- and microdiamonds by HPHT (high-pressure high-temperature) synthesis from organic substances. These two spit-vacancy complexes consist of impurity atoms located almost halfway between the two vacant sites in diamond lattice [Fig. 1(a)]. Ideally, the symmetry of the center is $\bar{3}m$. However, due to the incompletely filled doubly degenerate impurity electron level in the diamond band gap, this structure is Jahn-Teller unstable and the degeneracy should be lifted. Thus, the actual symmetry of the center should be lower, but EPR measurements clearly demonstrate the conservation of trigonal symmetry for both centers [18–20]. It is believed that the physical mechanism, which lifts this degeneracy in split-vacancy centers, is caused by the spin-orbit coupling [10,17,21]. So, the optical zero phonon line (ZPL), invoked by the promotion of electron from the lower e_u level to this incompletely filled e_g one (with energy difference between levels of about 1.68 eV for SiV^- and 2.05 for GeV^-), is split into quadruplet Z_{1-4} (see Fig. 1). The characteristic splitting energies in the GeV^- center reaches the value $\approx$4 meV. Oscillation of the heavy impurity atom gives rise to the local vibrational mode (LVM) in the diamond phonon spectrum, which is observed at $\approx$64 meV in SiV^- and $\approx$45 meV in GeV^- apart from the strongest component of the ZPL in the fluorescence sideband of these centers. Additional information on the structure and electronic properties of the split-vacancy complexes can be obtained through photoluminescence excitation (PLE) measurements, which can be regarded as a highly sensitive absorption technique [22]. Earlier, this research was carried out in the SiV^- center [23,24], but in a rather high-energy range, which involves excitation of lower electronic levels. However, PLE spectra in a range close to ZPL could provide valuable information on vibrational modes of impurity atom in split-vacancy complexes. Therefore, detailed analysis of these regions of PLE spectra could significantly enhance our understanding of the structure of these color centers in diamond.

The description of photon emission by impurity center is based on the Born-Oppenheimer approach where the fast electronic component is factorized from the slow atomic coordinates. Specifically, the matrix element of the dipole electronic transition between the final $\Psi_f(R,r)$ and initial $\Psi_i(R,r)$ states, where R and r denote impurity atom and its electrons coordinates, is written as

$$\int_R \int_r \Psi_i(r,R)\overline{\sigma}\Psi_f(r,R)dRdr \approx \int_r \psi_i(r)\overline{\sigma}\psi_f(r)dr \int_R \Phi_i(R)\Phi_f(R)dR.$$

Here $\psi(r)$ is an (multi)electron wave function independent on atomic coordinates, $\overline{\sigma}$ is a polarization vector of the emitted photon. This assumptions is known as the Franck-Condon approximation and for the allowed dipole electron transition (like the transition $e_g \rightarrow e_u$ in the split-vacancy complexes) it is believed to be enough. It can be experimentally demonstrated [25] that in the color centers in diamond the next term in decomposition on atomic coordinates (the Herzberg-Teller term) can be safely neglected. In $\int_R \ldots dR$ the integration is over coordinates of N atoms which in some way can "participate" in the electronic dipole transition. This includes atoms/ions the electron wave functions taking part in transition

*mkondrin@hppi.troitsk.ru

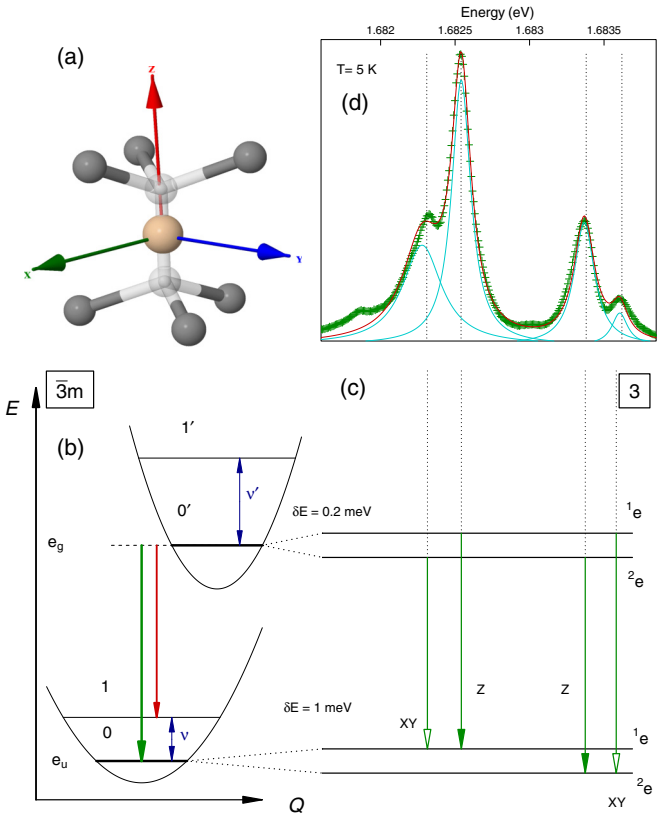

FIG. 1. (a) The structure of a split-vacancy complex in diamond. Dark gray balls stand for carbon atoms, translucent for vacant cites, and the large ball in the middle for an impurity atom. (b) Schematic representation of the Huang-Rhys model with the frequency defect. Tick marks throughout the text denote the excited electronic state. The arrows demonstrate the transitions corresponding to ZPL ($0' \rightarrow 0$) and the first LVM ($0' \rightarrow 1$) in the luminescence sideband. (c) Splitting of one electron energy levels due to symmetry breaking $\bar{3}m \rightarrow 3$. The open arrows represent transitions accompanied by the emission of $X(Y)$-polarized photons, the solid ones to Z-polarized ones. (d) The ZPL splitting of SiV^- center in the samples studied at designated temperature. ZPL is decomposed into four Lorentzians with the known separation in frequency. The polarization of individual ZPL components was attributed according to Ref. [10].

are spread over. In defect centers in diamond, besides proper impurity atom we should also include into this number at least its nearest-neighbor carbon atoms because in many cases the electrons that participate in optical transitions also form bonds with these adjacent carbon atoms. Additional simplifications in this notation are due to the fact that the impurity atom wave function $\Phi(R)$ can be well approximated by the wave function of a particle trapped in the more or less harmonic potential.

The normal mode can contribute to the ZPL sideband in two ways. First, the Stokes shift, a coordinate shift of the potential of the excited electronic state relative to the one of the ground state [Fig. 1(b)], could contribute to the ZPL only if the normal mode has a nonzero component along this shift. This is a very important restriction because in practice it turns out that only few (even only one) modes have to be considered. The second contribution of this mode to the luminescence sideband could originate from the frequency defect Δ, the difference between curvatures of potentials in the excited and the ground electron state. In harmonic approximation it can be conveniently expressed as the difference between oscillation quanta in the ground and the excited electronic states $\Delta = \nu' - \nu$. Such a mode produces LVMs located at frequencies ν and ν' relative to the ZPL in luminescence and absorption (or excitation) sidebands respectively with different intensities (governed by the frequency defect value). The frequency defect also gives rise to the splitting of ZPL into a series of satellites corresponding to the transitions between the oscillatory levels of ground and excited electronic states with the same oscillation quantum number. These satellites are located exactly Δ of their corresponding frequency defect away from the "true" ZPL (caused by transition $0 \rightarrow 0'$). Strictly speaking, these satellites are not vibrational modes because they are not accompanied by emission of phonons. Thus, they can be named phantom ZPLs. These lines are hard to register in experiments because the frequency defect as a rule is quite small (significantly less than either ν or ν'). However, the split-vacancy centers seems to serve as a remarkable exception, which gives one a chance to observe these phantom ZPLs.

In this research we have used combined PL/PLE optical measurements on GeV^- and SiV^- centers enforced by the previous data on isotopic shift observed in these centers and the first-principle calculations.

II. METHODS

For a description of a sample synthesis by HPHT treatment from hydrocarbons we refer the reader to the papers [4,17,26,27]. Microcrystals of up to 10–15 μm in size with perfect shape and nanocrystals of 50–300 nm in size are detected in as-synthesized samples. Isotopically pure germanium (^{73}Ge) and silicon with natural isotopic composition (≈92% ^{28}Si) were used as dopants.

Due to the very low concentration of impurity centers produced by the HPHT synthesis, no direct absorption measurements were possible. Instead we used more sensitive PLE method. PLE and optical absorption in general yield the same results, so these two experimental techniques are usually regarded as interchangeable [22]. PLE spectra were further considered as absorption spectra of split-vacancy centers.

Photoluminescence excitation and emission spectra were recorded with a FLSP920 spectrofluorometer (Edinburgh Instruments, UK) equipped with a low-noise microchannel plate photomultiplier. Diamond crystals were placed in a quartz tube (2.0 mm of inner diameter) and all photoluminescence experiments were performed in the reflective mode with a cylindrical quartz Dewar vessel at room temperature or 77 K. All obtained spectra were corrected for the wavelength-dependent sensitivity of the detection.

Low-temperature emission spectra were recorded with a grating spectrograph (Princeton Instruments SpectraPro 2500, 1200 grooves-per-mm grating) equipped with a Pylon charge-coupled device (CCD) detector (eXcelon, front illuminated). A spectral resolution better than 0.1 meV was provided by the entrance slit width of 20 μm and the same CCD pixel size. To obtain low-temperature (5 K) photoluminescence excitation spectra a grating monochromator (linear dispersion of 3.2 nm/mm) equipped with a tungsten lamp was used.

In most of the experiments, the spectral resolution of this excitation source was about 0.5 nm. Samples were immersed in the optical cryostat (Utreks1 RTA) and cooled by continuous flow of helium vapor. A steady-state semiconductor laser operating at a wavelength of 472 nm with power 40 mW was used as an excitation source. An approximately 2.5 times enlarged image of the excitation spot with an approximate size of 500 μm was focused at the entrance slit of the spectrograph using a quartz lens (100 nm focal length).

In *ab initio* calculations Quantum ESPRESSO software package was used [28]. Impurity center was modeled in 83-atoms periodic supercell having $P3$ symmetry. For the density functional calculation we employed the Perdew-Burke-Ernzerhof (PBE) exchange correlation method with norm-conserving pseudopotentials for both carbon and impurity atoms with the energy cutoff 70 Ry and the charge-density cutoff 800 Ry. For the integration over the Brillouin zone an unshifted $8 \times 8 \times 8$ Monkhorst-Pack grid was used. In the process of calculation the relaxation of cell dimensions and ions' positions (with initial symmetry fixed) was performed. Before the calculation of electronic states, the crystal lattices and atom positions were fully optimized until the residual force on every atom became less than 0.001 Ry/bohr. After that additional calculations were performed in the obtained geometry using hybrid (Heyd-Scuseria-Ernzerhof method) HSE06 functional to clarify the position of impurity levels and the electronic band gap. For this kind of calculation the energy sampling only in the center of the Brillouin zone was done. As it was shown earlier the hybrid functional calculations of impurity centers in diamond using the HSE06 method usually produce the excitation energy values close to the experimentally observed one [17,21,29,30].

Vibrational properties of the impurity atom was calculated by shifting the impurity atom along the Z axis or in the plane normal to it with the positions of all carbon atoms fixed. In this sort of calculation the "minimal" assumption about the ground and excited electronic states was adopted, that the local mode does not involve oscillation of carbon atom. For the local mode in the ground state this is suggested by the experimental evidence. For calculation of local modes only sampling in the Γ point of the Brillouin zone was performed.

The excited electronic state was modeled by inverse population of electronic states in the Γ point of the Brillouin zone (constrained density functional theory (DFT) method). So, the calculation required just several cycles of self-consistent *ab initio* runs. It is also interesting to note that although in these calculations only the PBE level of theory was used (generalized-gradient method with no nonlocal corrections) but the energy difference between the excited and the ground states obtained for an unshifted impurity atom closely reproduce the result obtained by the HSE06 method. So, this procedure for the description of electronic properties of defect centers provides a cheaper alternative to the much more computationally expensive HSE06 method.

III. RESULTS AND DISCUSSIONS

Let us consider the single SiV^- center. Luminescence of these centers was thoroughly studied in a number of works and it was found [10] that all four ZPL components have their own specific polarizations. In the ideal point group $\bar{3}m$ all polarizations are allowed, so this finding indicates that some sort of symmetry breaking takes place in this center. The observed polarization is best explained by symmetry breaking to the *3* point group (index 4 subgroup of $\bar{3}m$ point group) as shown in Figs. 1(c) and 1(d). Therefore, the symmetry breaking leads to the loss of inversion symmetry of the SiV^- center. This is also corroborated by the theoretical studies in Ref. [31] where it was proposed that the LVM component in a luminescence sideband has a_u symmetry (here the $\bar{3}m$ group is implied). The Stokes shift is possible only in the direction of the *ungerade* component [32]. Thus, the presence of a sideband line with such a symmetry indicates the certain type of structural distortion in the excited electronic state, which is, presumably, brought about by the loss of inversion symmetry produced by the slight shift of impurity atom along Z axis. Consequently, the two other degenerate vibrational modes, corresponding to the vibrations in the xy plane (e_u symmetry), do not contribute to the optical sideband at all. So, in this regard they can be named the silent modes.

It can be also demonstrated that the main component of the Stokes shift is just this displacement. Generally, it can be assumed that the distortion also influences adjacent carbon atoms. However, the experiments with isotopic substitution of impurity and carbon atoms [17] showed that only oscillations of the impurity atom are responsible for the LVM in an isostructural GeV^- center. Oscillations of carbon atoms have a negligible influence on the positions of these lines. Therefore, it is enough to consider only those modes, which involves oscillation of the impurity atom along the Z axis. It should be noted that in the three point group setting this type of oscillation is fully symmetric (it corresponds to the trivial representation A of this point group).

This approach in some way resembles one applied in Ref. [33] where the optical sideband of NV center in diamond was calculated from the first principles. However, in this work the frequency defect was assumed to be negligible. This is relevant to the NV center ($\Delta = 2$ and $\nu = 65$ meV) but it is not a general rule. It should be also stressed that at the moment DFT does not allow calculations of the vibrational properties of the lattice in the arbitrary electronic state (not the ground one). In particular, the absorption sideband can not be evaluated from the first principles without additional simplifying assumptions or some phenomenological parameters derived from experiment. In application to a particular impurity center in crystals these experimentally imposed assumptions can be very diverse. For example, in Ref. [34] on the basis of experimental findings it was proposed that an excited state of some impurity centers in GaN (which is also a wide-gap semiconductor as well as diamond) can be well approximated as an unexcited but differently charged state of the same centers. Although their assumptions are different from ours, they lead the authors to the conclusion of large frequency defects in these centers too.

The silent phonon modes accompanied with the frequency defect can be experimentally observed due to their contribution to the isotopic shift of the ZPL. Moreover, strong dependence of ZPL energy on the mass of an oscillating impurity atom is an unambiguous indication of the large frequency defect present in this center. We will illustrate this effect using a GeV^- center where the isotopic effects were thoroughly studied earlier

[17,26]. Assuming that the mass variation δm of the vibrating atom is small in comparison to the mass of the atom itself m, the Keil model [32] produces a simple approximate relation:

$$\frac{\delta Z}{\delta m} \approx \frac{-\Delta}{4m},$$

where δZ is the ZPL shift observed in the isotopic substitution of atoms involved in the electronic transition. Here we should regard

$$\Delta = \sum_{k=1}^{3N} \Delta_k$$

as a net frequency defect obtained by summations of individual frequency defects Δ_k of all $3N$ vibrational modes involved in the transition. The silent modes, which do not contribute to the sideband of the color center, are included too, as it was mentioned in the seminal paper on isotopic effects in diamond [35]. In other words Δ is the difference between the ground states of two $3N$ dimensional oscillators (corresponding to the excited and ground electronic states of impurity center) with varying curvatures along some of the coordinates (i.e., the corresponding mode has a frequency defect). By variation of the isotope mass of either the impurity atom or the carbon matrix one can independently measure either the frequency defects of the three modes corresponding to the impurity atom or the $3N - 3$ modes of the atoms in the diamond lattice. The frequency defect of the local mode visible in the sideband can be measured directly by comparison of the luminescence and absorption sidebands. Therefore, in the split-vacancy centers the frequencies of two other local modes, possessing the same frequency due to the trigonal symmetry of the center, can be extracted from the isotopic shift. Using the isotopic shift value $\delta Z/\delta m_{Ge} = -0.065$ meV/amu [26], the frequency defect of the fully symmetric A mode contributing to the optical sideband (with $\nu = 45$ meV) can be evaluated as $\Delta_A = 28$ meV, while the frequency defect of the two silent modes (with E symmetry) is $\Delta_E = -4$ meV (the negative sign means $\nu > \nu'$).

The isotopic substitution of a carbon atom in the crystal lattice has an additional side effect: it brings about the volume change of the lattice. For diamond the relative change on the $^{12}C \rightarrow {}^{13}C$ substitution [36–38] is about $\Delta V/V_0 \approx 5 \times 10^{-4}$. Using the known bulk modulus of diamond (≈500 GPa) and the experimental pressure coefficient of ZPL, this additional contribution (named the "static shift" in Collins *et al.* [35]) was evaluated [26] as only 0.8 meV out of 2.65 meV of the overall shift. The remaining 1.85 meV should be ascribed to the frequency defects of carbon atoms involved in the transition ("dynamic shift" according to Collins *et al.* [35]). Assuming that the three vibrational modes of the carbon atom have the same value of the frequency defect, it can be evaluated as −29 meV per mode. The similar argumentation and the right sign of the carbon frequency defect was earlier reported in Ref. [39].

The interplay between static and dynamic isotopic shifts produces the peculiar effect which consists in the change of splitting energies experimentally observed in these centers. The most vividly it demonstrates itself in the GeV$^-$ center where ^{12}C → ^{13}C substitution leads to diminishing of splitting energies by about 7% (Fig. 2).

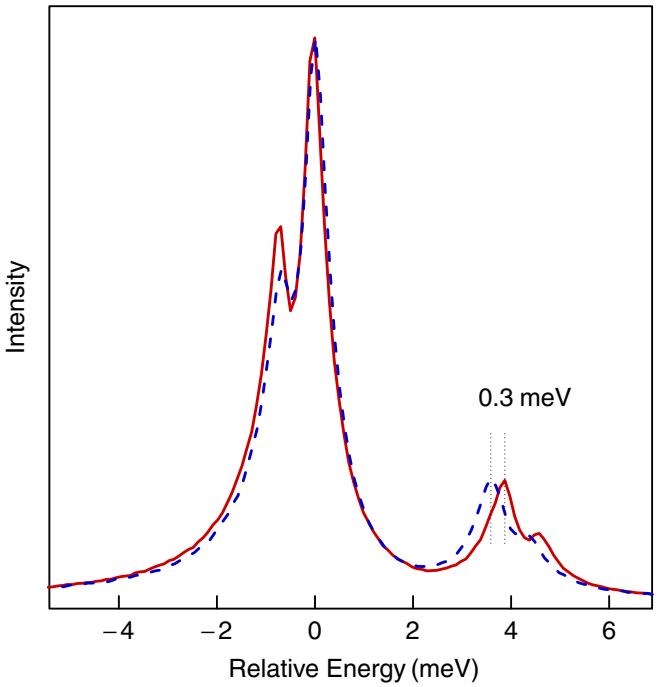

FIG. 2. ZPL slitting of GeV$^-$ center in ^{12}C (solid line) and ^{13}C (dashed line) diamonds. The spectra were shifted by 2.0622 and 2.0593 eV for ^{13}C and ^{12}C respectively.

Now we consider the phantom ZPL present in the split-vacancy centers. In principle, any mode with a large enough frequency defect can produce such a line. However, the intensity of this line is controlled by the population of the first oscillation level in the ground state. Therefore, at low temperatures only the modes with small ν can be observed. In the GeV$^-$ center these conditions are satisfied for the A mode [26] (the same which produce the LVM in photoluminescence sideband); see Fig. 3. Thus, in the PLE (or absorption) sideband at liquid-nitrogen temperatures this mode contributes twice: first as a phantom ZPL at $\Delta_A = 28$ meV apart from the true ZPL and as a LVM at $\nu' = 73$ meV.

Of course, these arguments do not necessarily rule out possible anharmonicity effects in the optical transition in the GeV$^-$ center proposed earlier [26]. However, the experimental data obtained on PL/PLE measurements of the SiV$^-$ center demonstrates that anharmonicity is not the main factor in the split-vacancy complexes.

The PL/PLE spectra of SiV$^-$ center in the vicinity of the ZPL at low ($T = 4.5$ K) and intermediate ($T = 77$ K) temperatures are shown in Fig. 3. The peaks marked by $P_{1\text{–}6}$ correspond to bulk phonon modes and they are usually observed in color centers in diamond [26,40]. The LVM in the PL and PLE sidebands have slightly different energies, $\nu' = 78$ meV and $\nu = 64$ meV, so its frequency defect is not significant. However, the phantom ZPL with similar energy, $\Delta = 14.5$ meV, is observed in the PLE spectrum at $T = 77$ K. At low temperatures this line is extinguished.

To complete the analysis we need the value of the isotopic shift in SiV$^-$ center $\delta Z/\delta m_{Si} = -0.33$ meV/amu [6,41]. It was demonstrated [41] that the energy of the local mode in photoluminescence scales as $1/\sqrt{m_{Si}}$, which proves that this

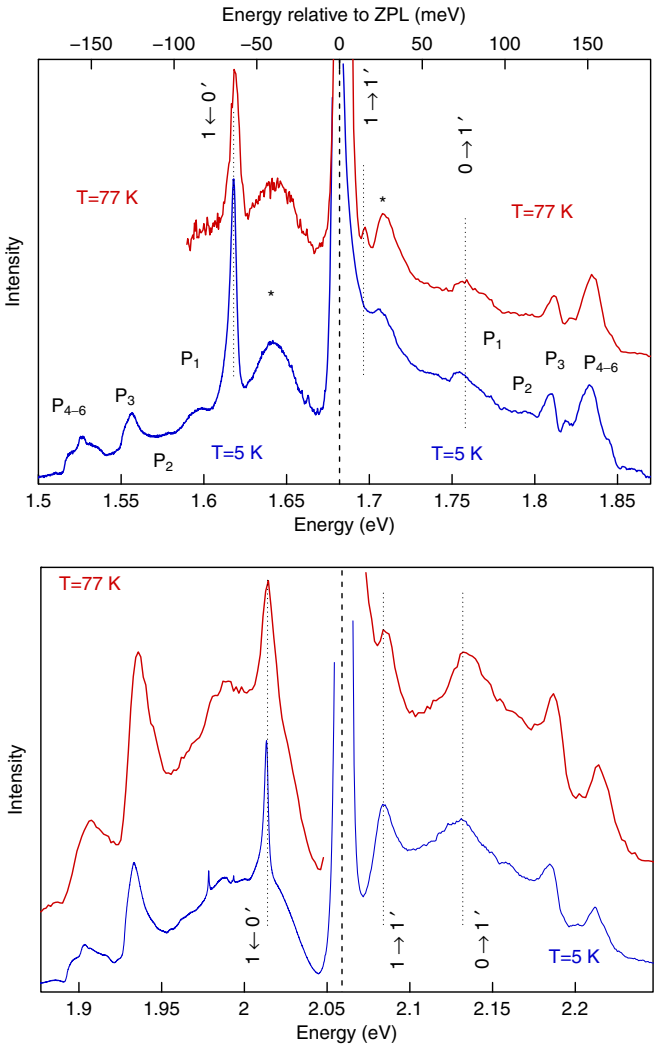

FIG. 3. PL/PLE spectra of SiV^- (upper panel) and GeV^- (lower panel) centers at intermediate ($T = 77$ K) and low ($T = 5$ K) temperatures. Both panels have the same x-axis scales, which were selected for visual coincidence of respective ZPLs (marked by vertical dashed line). PL and PLE spectra correspond to energies lower and higher than the ZPL one respectively. Asterisks mark the positions of the background maximum in both emission and absorption sidebands.

mode (similarly to GeV^- center) is due to the oscillation of the impurity atom alone. Thus, the frequency defect of the other two silent E modes of the impurity atom can be evaluated as ≈11.5 meV. The corresponding phantom ZPL is not observed in the PLE sideband, probably due to the higher energy of E modes in comparison to the energy of the A mode ($\nu = 65$ meV). So, it is extinguished due to depopulation of the first oscillatory level at liquid-nitrogen temperatures. The higher energy of the E quasilocal modes is also predicted by DFT calculations [42] where the energy of the e_u mode in the ground electronic state was evaluated as ∼100 meV. Experimental findings enable us to evaluate the binding energies of the SiV^- center. Particularly, we make no hypothesis about vibronic properties in the excited and ground electronic states. Instead we rely upon the experimental evidence that the vibronic sideband is mostly due to the

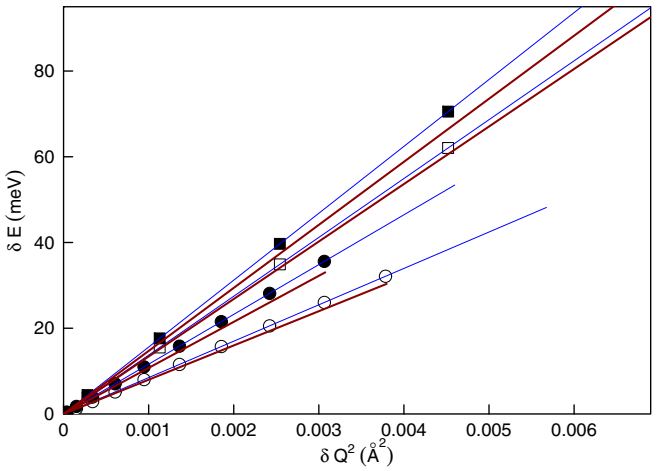

FIG. 4. Calculated relative energies of SiV^- center depending on the displacement of impurity atom along Z axis (○) and in XY plane (□). Filled symbols correspond to the excited electronic state and the open ones to the ground electronic state. The thick lines represent the calculated energies of GeV^- center in comparison to SiV^-.

oscillation of the heavy impurity atom alone. Therefore, the oscillation quantum could be calculated taking into account only shifting the impurity atom and fixing coordinates of all carbon atoms. The cross sections of a potential surface obtained in such a way, that enables one to evaluate the local vibrational modes of impurity atom, are presented in Fig. 4. The oscillation quanta $\Delta\varepsilon$ can be obtained using the corresponding coefficient $\frac{\delta E}{\delta q^2}$ from Fig. 4 and the well-known formula (here M is the mass of the impurity atom)

$$\Delta\varepsilon = \hbar\sqrt{\frac{2}{M}\frac{\delta E}{\delta q^2}}.$$

The calculated vibrational energies are shown in Table I. Although the energies of vibrational modes are significantly underestimated, probably due to the small size of computational supercell, in this calculation we have caught important features of split-vacancy centers in diamond. These features are the positive frequency defects of local vibrational modes and significantly higher energies of oscillations in the xy plane (E modes) in comparison to oscillations along the Z axis (A mode). It is also worth noting that this calculation predicts

TABLE I. Energies (in meV) of calculated local vibrational modes in split-vacancy centers. $\Delta = 2(XY' - XY) + (Z' - Z)$ is a net frequency defect of impurity atom. I_{1-2} and $\tilde{I}_{1-2}$: experimental and calculated by HSE06 method values (in eV) of the first and the second excited electronic values respectively. The values in parentheses are corresponding excitation energies calculated by the constrained DFT method in PBE approximation.

	Z	XY	Z'	XY'	Δ	I_1	I_2	$\tilde{I}_1$	$\tilde{I}_2$
SiV^-	50.2	63.8	58.7	68.1	17.0	1.683	2.271	1.613 (1.672)	2.133 (2.289)
GeV^-	30.3	39.3	35.2	41.2	8.5	2.059	2.772	1.922 (1.995)	2.311 (2.541)

that the energy of local modes in SiV and GeV centers scales practically as a square root of the impurity atom mass. This trend was already mentioned in Refs. [4,40].

DFT calculation fully corroborates the experimental findings: the higher oscillation energies of the ground electronic state in the XY plane than along the Z axis and intermediate oscillation energies along the Z axis in the excited electronic state in comparison to that in the ground one. The difference between the last two values demonstrates the positive frequency defect, which we suppose to be pertinent for the split-vacancy centers.

The attribution of vibrational modes in the SiV^- center is very complicated due to the presence of an additional line at 720 nm observed in these centers. In the recent research it was usually attributed either to boron complexes [19,43] or to more complicated structural defects. In any case, it can be demonstrated that this line is not associated with the proper SiV^- center, because its excitation requires significantly larger energies than were used in our PLE experiments. So, we consider this line to be not relevant to the observed peaks in the high-energy sideband of the SiV^- center.

The experimental shift value of the SiV^- center caused by isotopic substitution of carbon atoms $\delta Z/\delta m_C$ is equal to 1.85 meV/amu [44] and the dynamic isotope shift was evaluated as 1.65 meV ($\delta Z/\delta P$ is three times less in SiV^- than in GeV^-). So, it is practically the same as in the GeV^- center (1.85 meV). Presumably, the dynamic shift for isostructural defects should be more or less invariant, because this implies that the same number of carbon atoms take part in the optical transition. If one also assumes that the average frequency defect of carbon atom is the same in diamond, then, by comparison of $\delta Z/\delta m_C$ in different optical centers, we can tell the relative number of carbon atom involved in optical transitions. For example, for the well-known NV^- center the corresponding ZPL shift values are $\delta Z/\delta m_C = 2.1$ meV/amu [39] and $\delta Z/\delta P = 5.5$ meV/GPa [45,46]. This yields the dynamic shift value 0.75 meV that is almost two times lower than in GeV^- and SiV^- centers. Therefore we can conclude that the number of carbon atoms participating in optical transition in split-vacancy centers is almost twice as much as that in the NV^- one. It means that in impurity-vacancy centers the wave function of the electron taking part in optical transitions is distributed over the nearest-neighbor carbon atoms with which the impurity atom has the chemical bonds (six in split-vacancy centers and three in NV^-).

The PLE technique can also be applied to investigate the impurity levels located deeply in the valence band. The ZPL discussed so far corresponds to electron transition from the impurity e_g doublet in the band gap and e_u doublet just below the valence band top. Here the $\bar{3}m$ point group is implied. In both centers this last energy level is about 10 meV deep in the valence zone and the impurity level in the band gap is 1.62 and 1.95 eV above the valence band top for SiV and GeV centers respectively. Because the e_u impurity doublet is in resonance with the T_g level which in pure diamond constitutes the top of the valence band, the last is split into $T_g \rightarrow A_{1g} + E_g$ (the last two representations correspond to $\bar{3}m$ symmetry). The first singlet forms the valence-band maximum and the second doublet is approximately 550 meV below it

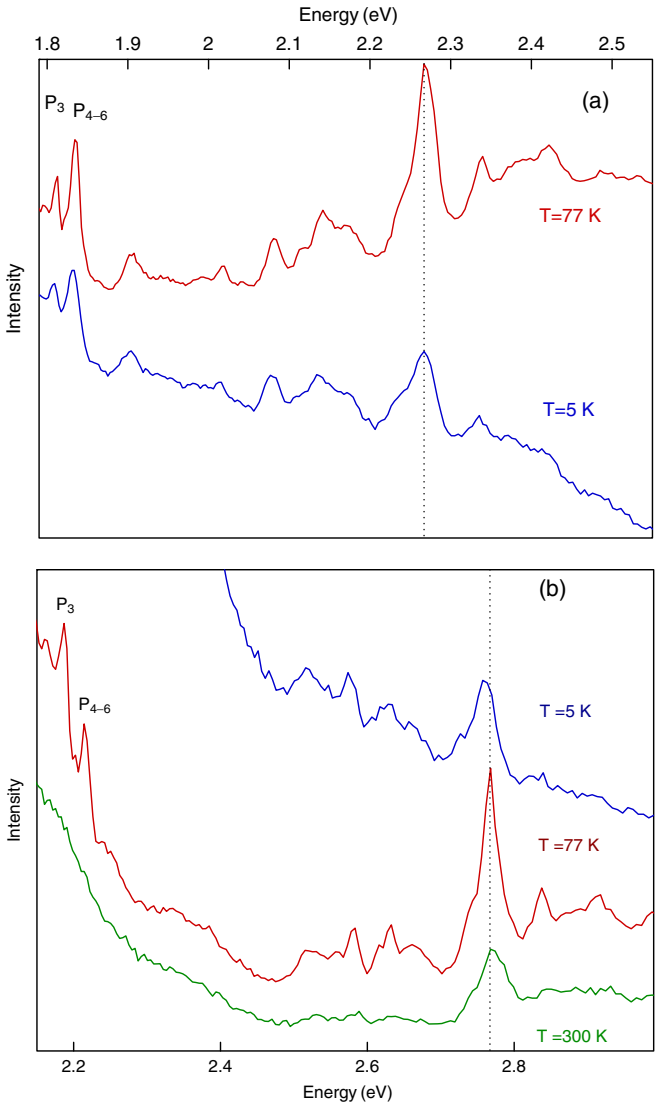

FIG. 5. PLE spectra of SiV^- (a) and GeV^- (b) in the excitation region far from ZPL at several temperatures. The strongest line observed in this region (marked by dotted lines) is possibly due to the excitation from the electronic level laying deep into the valence band and subsequent complicated relaxation of the obtained excited state [24]. Weak lines in the vicinity of it are likely to be its vibronic replicas and strongly attenuates at room temperature.

(independent on the type of impurity atom). The promotion of the electron from this level to the partially filled one in the band gap produces the second excited state experimentally observed earlier in these centers [24]. The transition $E_g \rightarrow E_g$ is forbidden, but due to the symmetry breaking this restriction is relaxed. The decay of the second excited state formed by promotion of electrons from these deep levels produces sharp peaks observed in the far PLE energy range (see Fig. 5, and Ref. [24]). In contrast to the data reported in Ref. [24], our low-temperature measurements enable us to precisely estimate the energies of this second excited state and demonstrate that the experimental values significantly differ from the calculated ones. The DFT predicts that the second excited level should be about 550 meV higher than the first one (corresponding to

the ZPL energy) in both SiV^- and GeV^- centers. Obviously, this contradicts the experimental observation (Fig. 5) and the dependence of the energy on the impurity atom type does exist. Note that there are two decay channels for the second excited state. First, the electron can be directly transferred to the ground state, with the emission of a single photon with the energy 2.3–2.6 eV. The second channel is a two-stage transition with the emission of photons of corresponding energy: (a) from the second to the first excited state and then (b) from the first excited state to the ground state ($E_g \rightarrow E_u$). The last channel contributes to the ZPL observed in these color centers, so it can be registered by PLE technique applied in our work. Probably, the complicated character of relaxation of the second excited electronic state is reflected in the complex photoluminescence decay (which involves three characteristic times) observed in the GeV^- center, excited by the short-wave excitation ($\lambda_{exc} = 375$ nm) [47].

IV. CONCLUSIONS AND FINAL REMARKS

Impurity centers in solid-state matrix resemble very much individual atoms and molecules, which significantly simplifies their theoretical description. However, the fact that these centers are embedded in crystal structures, where the empty space is limited, leads to even further simplification. So it turns out that in crystal lattice there are very few directions where the excited impurity atom can be shifted and produce an optical vibrational mode in the sideband of the luminescence ZPL. The crystal symmetry of the solid-state matrix induces possible displacement of the impurity atom. In particular, the Duschinsky effect consisting in rotation of symmetry axis of molecules in the ground and excited electronic states seems to be almost impossible in the solid-state impurity centers. Thus, the "parallel-mode approximation" [34] seems to be the most viable option. In this case one can assume that the distortion of the impurity atom takes place in the direction of the softest vibrational mode. Just this effect is observed in two defect centers in diamond described in this work. In this regard the diamond crystal composed of light atoms bound by strong covalent forces can be considered as a convenient model system where local vibrations of heavier (in comparison to carbon) impurity atoms can be studied in a rather large energy window (≈70 meV, the energy corresponding to the transverse acoustical mode on the Brillouin-zone edge of pure diamond).

On the other hand, the limited free space produced by two adjacent vacancies in diamond lattice also leads to another peculiar effect which seems to be common to the atoms with large atomic radius (Si, Ge, etc). They do not fit well into a produced void so electronic excitation leads to an increase of binding energy and subsequently a large frequency defect. The obvious counterexample is NV^- centers where the frequency defect is negligible. However, the nitrogen atom also has the smallest atomic radius.

We conclude that the combined PL/PLE experimental methods and isotopic shift measurements enhance understanding of the structure of the impurity-vacancy centers. It was demonstrated that the difference between the photoluminescence and absorption optical sidebands observed in the temperature range 5–77 K in the isostructural SiV^- and GeV^- centers can be best explained by the frequency defect present in this center. The experimental observations are corroborated by the first-principle calculations which predict a significant frequency defect for local vibrational modes of split-vacancy centers in diamond.

ACKNOWLEDGMENTS

This work was supported by Russian Foundation for Basic Research Grants No. 17-52-50075 and No. 15-02-05603. Photoluminescence excitation measurements were supported by Federal Agency of Scientific Organizations Russia (Project No. 0333-2016-0001). The helpful comments from S. N. Nikolaev are acknowledged.

[1] A. Sipahigil, R. E. Evans, D. D. Sukachev, M. J. Burek, J. Borregaard, M. K. Bhaskar, C. T. Nguyen, J. L. Pacheco, H. A. Atikian, C. Meuwly, R. M. Camacho, F. Jelezko, E. Bielejec, H. Park, M. Lončar, and M. D. Lukin, Science **354**, 847 (2016).

[2] M. K. Bhaskar, D. D. Sukachev, A. Sipahigil, R. E. Evans, M. J. Burek, C. T. Nguyen, L. J. Rogers, P. Siyushev, M. H. Metsch, H. Park, F. Jelezko, M. Lončar, and M. D. Lukin, Phys. Rev. Lett. **118**, 223603 (2017).

[3] P. Siyushev, M. H. Metsch, A. Ijaz, J. M. Binder, M. K. Bhaskar, D. D. Sukachev, A. Sipahigil, R. E. Evans, C. T. Nguyen, M. D. Lukin, P. R. Hemmer, Y. N. Palyanov, I. N. Kupriyanov, Y. M. Borzdov, L. J. Rogers, and F. Jelezko, Phys. Rev. B **96**, 081201 (2017).

[4] E. A. Ekimov and M. V. Kondrin, Phys. Usp. **60**, 539 (2017).

[5] V. S. Vavilov, A. A. Gippius, A. M. Zaitsev, B. V. Deryagin, B. V. Sinitsyn, and A. E. Alekseenko, Fiz. Tekh. Poluprovodn. **14**, 1811 (1980) (in Russian) [Sov. Phys. Semicond. **14**, 1078 (1980)].

[6] C. D. Clark, H. Kanda, I. Kiflawi, and G. Sittas, Phys. Rev. B **51**, 16681 (1995).

[7] J. P. Goss, R. Jones, S. J. Breuer, P. R. Briddon, and S. Öberg, Phys. Rev. Lett. **77**, 3041 (1996).

[8] J. P. Goss, P. R. Briddon, M. J. Rayson, S. J. Sque, and R. Jones, Phys. Rev. B **72**, 035214 (2005).

[9] C. Hepp, T. Müller, V. Waselowski, J. N. Becker, B. Pingault, H. Sternschulte, D. Steinmüller-Nethl, A. Gali, J. R. Maze, M. Atatüre, and C. Becher, Phys. Rev. Lett. **112**, 036405 (2014).

[10] L. J. Rogers, K. D. Jahnke, M. W. Doherty, A. Dietrich, L. P. McGuinness, C. Müller, T. Teraji, H. Sumiya, J. Isoya, N. B. Manson, and F. Jelezko, Phys. Rev. B **89**, 235101 (2014).

[11] L. J. Rogers, K. D. Jahnke, M. H. Metsch, A. Sipahigil, J. M. Binder, T. Teraji, H. Sumiya, J. Isoya, M. D. Lukin, P. Hemmer, and F. Jelezko, Phys. Rev. Lett. **113**, 263602 (2014).

[12] H. Zhang, I. Aharonovich, D. R. Glenn, R. Schalek, A. P. Magyar, J. W. Lichtman, E. L. Hu, and R. L. Walsworth, Small **10**, 1908 (2014).

[13] I. Aharonovich and E. Neu, Adv. Opt. Mater. **2**, 911 (2014).
[14] T. Iwasaki, F. Ishibashi, Y. Miyamoto, Y. Doi, S. Kobayashi, T. Miyazaki, K. Tahara, K. D. Jahnke, L. J. Rogers, B. Naydenov, F. Jelezko, S. Yamasaki, S. Nagamachi, T. Inubushi, N. Mizuochi, and M. Hatano, Sci. Rep. **5**, 12882 (2015).
[15] Y. N. Palyanov, I. N. Kupriyanov, Y. M. Borzdov, and N. V. Surovtsev, Sci. Rep. **5**, 14789 (2015).
[16] V. G. Ralchenko, V. S. Sedov, A. A. Khomich, V. S. Krivobok, S. N. Nikolaev, S. S. Savin, I. I. Vlasov, and V. I. Konov, Bull. Lebedev Phys. Inst. **42**, 165 (2015).
[17] E. A. Ekimov, S. G. Lyapin, K. N. Boldyrev, M. V. Kondrin, R. Khmelnitskiy, V. A. Gavva, T. V. Kotereva, and M. N. Popova, JETP Lett. **102**, 701 (2015).
[18] A. M. Edmonds, M. E. Newton, P. M. Martineau, D. J. Twitchen, and S. D. Williams, Phys. Rev. B **77**, 245205 (2008).
[19] V. Nadolinny, A. Komarovskikh, Y. Palyanov, I. Kupriyanov, Y. Borzdov, M. Rakhmanova, O. Yuryeva, and S. Veber, Phys. Status Solidi A **213**, 2623 (2016).
[20] A. Komarovskikh, A. Dmitriev, V. Nadolinny, and Y. Palyanov, Diam. Relat. Mater. **76**, 86 (2017).
[21] A. Gali and J. R. Maze, Phys. Rev. B **88**, 235205 (2013).
[22] K. Iakoubovskii and G. Davies, Phys. Rev. B **70**, 245206 (2004).
[23] K. Iakoubovskii and G. J. Adriaenssens, Phys. Rev. B **61**, 10174 (2000).
[24] S. Häussler, G. Thiering, A. Dietrich, N. Waasem, T. Teraji, J. Isoya, T. Iwasaki, M. Hatano, F. Jelezko, A. Gali, and A. Kubanek, New J. Phys. **19**, 063036 (2017).
[25] E. A. Ekimov, V. S. Krivobok, S. G. Lyapin, P. S. Sherin, V. A. Gavva, and M. V. Kondrin, *Nanosystems: Physics, Chemistry, Mathematics* (in press).
[26] E. A. Ekimov, V. S. Krivobok, S. G. Lyapin, P. S. Sherin, V. A. Gavva, and M. V. Kondrin, Phys. Rev. B **95**, 094113 (2017).
[27] V. A. Davydov, A. V. Rakhmanina, S. G. Lyapin, I. D. Ilichev, K. N. Boldyrev, A. A. Shiryaev, and V. N. Agafonov, JETP Lett. **99**, 585 (2014).
[28] P. Giannozzi, S. Baroni, N. Bonini, M. Calandra, R. Car, C. Cavazzoni, D. Ceresoli, G. L. Chiarotti, M. Cococcioni, I. Dabo, A. D. Corso, S. de Gironcoli, S. Fabris, G. Fratesi, R. Gebauer, U. Gerstmann, C. Gougoussis, A. Kokalj, M. Lazzeri, L. Martin-Samos *et al.*, J. Phys.: Condens. Matter **21**, 395502 (2009).
[29] A. Gali, M. Fyta, and E. Kaxiras, Phys. Rev. B **77**, 155206 (2008).
[30] A. Gali, E. Janzén, P. Deák, G. Kresse, and E. Kaxiras, Phys. Rev. Lett. **103**, 186404 (2009).
[31] A. Norambuena, S. A. Reyes, J. Mejía-Lopéz, A. Gali, and J. R. Maze, Phys. Rev. B **94**, 134305 (2016).
[32] T. H. Keil, Phys. Rev. **140**, A601 (1965).
[33] A. Alkauskas, B. B. Buckley, D. D. Awschalom, and C. G. Van de Walle, New J. Phys. **16**, 073026 (2014).
[34] A. Alkauskas, J. L. Lyons, D. Steiauf, and C. G. Van de Walle, Phys. Rev. Lett. **109**, 267401 (2012).
[35] A. Collins, G. Davies, H. Kanda, and G. S. Woods, J. Phys. C **21**, 1363 (1988).
[36] H. Holloway, K. C. Hass, M. A. Tamor, T. R. Anthony, and W. F. Banholzer, Phys. Rev. B **44**, 7123 (1991).
[37] M. Muinov, H. Kanda, and S. M. Stishov, Phys. Rev. B **50**, 13860 (1994).
[38] P. Gillet, G. Fiquet, I. Daniel, B. Reynard, and M. Hanfland, Phys. Rev. B **60**, 14660 (1999).
[39] G. Davies, Physica B (Amsterdam) **273-274**, 15 (1999).
[40] A. M. Zaitsev, Phys. Rev. B **61**, 12909 (2000).
[41] A. Dietrich, K. D. Jahnke, J. M. Binder, T. Teraji, J. Isoya, L. J. Rogers, and F. Jelezko, New J. Phys. **16**, 113019 (2014).
[42] E. Londero, G. Thiering, M. Bijeikytè, J. R. Maze, A. Alkauskas, and A. Gali, arXiv:1605.02955.
[43] V. S. Sedov, V. S. Krivobok, A. V. Khomich, V. G. Ralchenko, A. A. Khomich, A. K. Martyanov, S. N. Nikolaev, O. N. Poklonskaya, and V. I. Konov, J. Appl. Spectrosc. **83**, 229 (2016).
[44] V. Sedov, K. Boldyrev, V. Krivobok, S. Nikolaev, A. Bolshakov, A. V. Khomich, A. A. Khomich, A. Krasilnikov, and V. Ralchenko, Phys. Status Solidi A **214**, 1700198 (2017).
[45] M. Kobayashi and Y. Nisida, Jpn. J. Appl. Phys. **32**, 279 (1993).
[46] M. W. Doherty, V. V. Struzhkin, D. A. Simpson, L. P. McGuinness, Y. Meng, A. Stacey, T. J. Karle, R. J. Hemley, N. B. Manson, L. C. L. Hollenberg, and S. Prawer, Phys. Rev. Lett. **112**, 047601 (2014).
[47] A. Komarovskikh, V. Nadolinny, V. Plyusnin, Y. Palyanov, and M. Rakhmanova, Diam. Relat. Mater. **79**, 145 (2017).